

Krylov Model-Order Reduction Expansions for Electromagnetic Wave Fields in Strongly Resonating Structures

J. T. Zimmerling*

R. F. Remis*

Abstract — In this paper we demonstrate the effectiveness of Krylov subspace model-order reduction techniques to simulate wave field propagation in strongly resonating structures. By utilizing an optimal complex-scaling method that simulates the extension to infinity, we show that Krylov reduction allows for effective wave field computations and dominant open resonant modes can be obtained at negligible additional costs as well. A number of numerical examples illustrate the performance of the proposed Krylov reduced-order modeling technique.

1 INTRODUCTION

In this paper we demonstrate the effectiveness of Krylov subspace model-order reduction techniques to simulate wave field propagation in strongly resonating structures. By utilizing an optimal complex-scaling method that simulates the extension to infinity, we show that Krylov reduction in combination with a stability-correction procedure allows for effective wave field computations.

The complex scaling method was proposed already in the 1970s (see, for example, [1] – [3]) and can be seen as a variant of the perfectly matched layer technique. In [4] this method was refined and a global and optimal complex scaling method for domain truncation was proposed (see [5] for further improvements). However, the problem with complex scaling is that causality is lost. Fortunately, stable time-domain or conjugate-symmetric frequency-domain solutions can still be constructed, provided that a stability-correction procedure is applied [4]. In addition, the scaled Maxwell system matrix can be shown to be complex-symmetric with respect to a certain bilinear form for instantaneously reacting media [6] as well as for media exhibiting relaxation [7]. This symmetry property enables us to efficiently compute Krylov subspace reduced-order models for the electromagnetic field via a three-term Lanczos-type reduction algorithm. Furthermore, with the help of the Lanczos algorithm we are able to identify the dominant open resonant modes that are

excited by the external current source. The number of these modes is typically very small for resonating structures and the electromagnetic field can therefore be computed very efficiently provided the resonant modes are quickly captured by a Krylov reduction method.

2 BASIC EQUATIONS AND REDUCED-ORDER MODELING

We consider electromagnetic wave propagation in instantaneously reacting media or media exhibiting first- or second-order dielectric relaxation effects. In both cases, the electromagnetic field is governed by the Maxwell equations

$$-\nabla \times \mathbf{H} + \partial_t \mathbf{D} = -\mathbf{J}^{\text{ext}} \quad (1)$$

and

$$\nabla \times \mathbf{E} + \mu_0 \partial_t \mathbf{H} = \mathbf{0}, \quad (2)$$

where $\mathbf{D} = \varepsilon \mathbf{E} + \tilde{\mathbf{P}}$ with $\varepsilon = \varepsilon_0 \varepsilon_\infty$ and ε_∞ is the instantaneous (high frequency) relative permittivity. For instantaneously reacting materials $\tilde{\mathbf{P}} = \varepsilon_0 \mathbf{E}$, while for matter exhibiting first- or second-order relaxation effects (Debye, Drude, or Lorentz materials), $\tilde{\mathbf{P}}$ is related to the electric field strength via a first- or second-order differential equation in time. For example, for a Drude material we have the constitutive relation

$$\partial_t^2 \tilde{\mathbf{P}} + \gamma_p \partial_t \tilde{\mathbf{P}} = \varepsilon_0 \omega_p^2 \mathbf{E}, \quad (3)$$

where γ_p is the collision frequency and ω_p the volume plasma frequency of the material.

Introducing the auxiliary field $\mathbf{U} = -\partial_t \tilde{\mathbf{P}}$, we can write Maxwell's equations and the constitutive relation in first-order form as

$$(\mathcal{D} + \mathcal{S} + \mathcal{M} \partial_t) \mathcal{F} = -\mathcal{Q}', \quad (4)$$

where \mathcal{D} is the spatial differential operator, \mathcal{S} and \mathcal{M} are medium matrices, \mathcal{F} is the field vector, and \mathcal{Q}' is the source vector. We only consider source vectors of the form $\mathcal{Q}' = w(t) \mathcal{Q}$, where $w(t)$ is the source signature that vanishes for $t < 0$ and \mathcal{Q} is time-independent.

*Circuits and Systems Group, Faculty of Electrical Engineering, Mathematics and Computer Science, Delft University of Technology, Mekelweg 4, 2628 CD Delft, The Netherlands, e-mail: J.T.Zimmerling@tudelft.nl, R.F.Remis@tudelft.nl

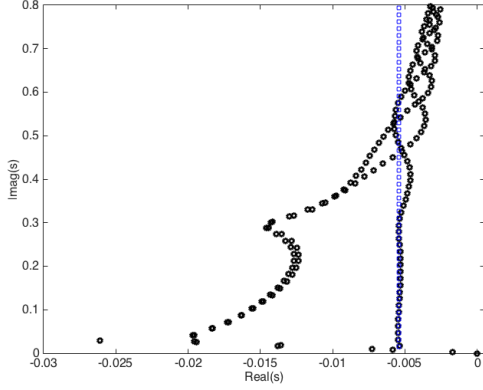


Figure 1: Normalized analytic (blue squares) and computed (black circles) open resonances of a one-dimensional slab.

Subsequently, we discretize the above first-order Maxwell system in space on a staggered Yee grid and use an optimal complex scaling method to simulate the extension to infinity (a variant of the perfectly matched layer technique, see [1] – [5] for details). After this discretization procedure, we arrive at the state-space representation

$$(\mathbf{D} + \mathbf{S} + \mathbf{M}\partial_t)\mathbf{f}_{cs} = -w(t)\mathbf{q}. \quad (5)$$

This system is complex and unstable due to the application of the complex scaling method. However, by applying the stability correction procedure described in [4], stable time-domain field approximations can be computed from this system as

$$\mathbf{f}(t) = -w(t) * 2\eta(t)\text{Re}[\eta(\mathbf{A})\exp(-\mathbf{A}t)\mathbf{M}^{-1}\mathbf{q}], \quad (6)$$

where the asterisk denotes convolution in time, $\mathbf{A} = \mathbf{M}^{-1}(\mathbf{D} + \mathbf{S})$ is the system matrix, and

$$\eta(z) = \begin{cases} 1 & \text{if } \text{Re}(z) > 0 \\ 0 & \text{if } \text{Re}(z) < 0 \end{cases} \quad (7)$$

is the complex Heaviside unit step function. Furthermore, the system matrix \mathbf{A} is complex-symmetric with respect to the bilinear form

$$\langle \mathbf{x}, \mathbf{y} \rangle = \mathbf{y}^T \mathbf{W} \mathbf{M} \mathbf{x}, \quad (8)$$

where \mathbf{W} is a step size matrix having certain products of the step sizes of the computational grid as its elements [7]. Now assuming that the system matrix is diagonalizable, the field vector can be written as

$$\mathbf{f}(t) = -w(t) * 2\eta(t)\text{Re}\left[\sum_{j=1}^n \alpha_j \eta(\lambda_j) \exp(-\lambda_j t) \mathbf{s}_j\right], \quad (9)$$

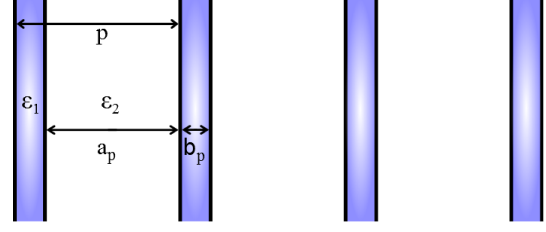


Figure 2: Part of a finite one-dimensional photonic crystal.

where n is the order of matrix \mathbf{A} , λ_j and \mathbf{s}_j are the eigenvalues and corresponding eigenvectors of this matrix, and $\alpha_j = \langle \mathbf{s}_j, \mathbf{M}^{-1}\mathbf{q} \rangle$. How many modes essentially contribute to the electromagnetic wave field on a given time interval depends on the configuration of interest, of course.

Finally, by exploiting the symmetry of the system matrix with respect to the bilinear form of Eq. (8), we can construct Krylov subspace reduced-order models for the electromagnetic field via an efficient Lanczos-type three-term recursion algorithm [4]. With the source vector $\mathbf{M}^{-1}\mathbf{q}$ as a starting vector, this algorithm produces a basis for a Krylov subspace generated by the system matrix and the source vector $\mathbf{M}^{-1}\mathbf{q}$ and after $m \ll n$ iterations we have the summarizing equation

$$\mathbf{A}\mathbf{V}_m = \mathbf{V}_m \mathbf{H}_m + \mathbf{r}_m \mathbf{e}_m^T, \quad (10)$$

where the n -by- m matrix $\mathbf{V}_m = (\mathbf{v}_1, \mathbf{v}_2, \dots, \mathbf{v}_m)$ has the Krylov subspace basis vectors \mathbf{v}_i as its columns and \mathbf{H}_m is an m -by- m tridiagonal matrix containing the recurrence coefficients of the Lanczos algorithm. Finally, \mathbf{r}_m is a residual vector and \mathbf{e}_m is the m th column of the m -by- m identity matrix. Based on the decomposition of Eq. (10) we can construct the reduced-order models

$$\begin{aligned} \mathbf{f}_m(t) = & \\ & -w(t) * 2\|\mathbf{M}^{-1}\mathbf{q}\|\eta(t)\text{Re}[\mathbf{V}_m \eta(\mathbf{H}_m) \exp(-\mathbf{H}_m t) \mathbf{e}_1] \end{aligned} \quad (11)$$

and dominant open resonant modes can be determined from Eq. (10) as well. Specifically, if (θ_i, \mathbf{x}_i) is an eigenpair of the tridiagonal matrix \mathbf{H}_m then postmultiplication of Eq. (10) by \mathbf{x}_i leads to

$$\mathbf{A}\mathbf{z}_i = \theta_i \mathbf{z}_i + \mathbf{r}_m \mathbf{e}_m^T \mathbf{x}_i, \quad (12)$$

where $\mathbf{z}_i = \mathbf{V}_m \mathbf{x}_i$. Equation (12) shows that if $\|\mathbf{e}_m^T \mathbf{x}_i\| \|\mathbf{r}_m\|$ is small then (θ_i, \mathbf{z}_i) is an approximate eigenpair of the system matrix \mathbf{A} . Note that $\|\mathbf{e}_m^T \mathbf{x}_i\| \|\mathbf{r}_m\|$ can be computed directly and it is therefore easily checked whether an eigenpair of matrix \mathbf{H}_m has converged to an eigenpair of matrix \mathbf{A} .

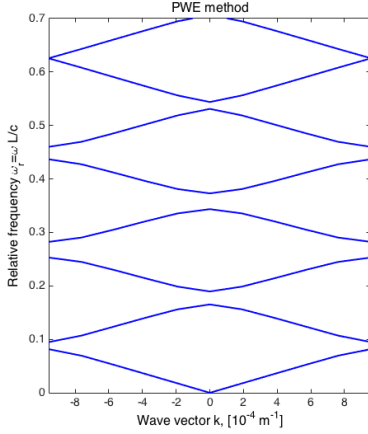


Figure 3: Bandgap structure on the first Brillouin zone of the infinite 1D photonic crystal that corresponds to the finite crystal of Figure 2. The bandgap structure is computed via the plane wave expansion method.

3 NUMERICAL RESULTS

As a first example, we consider a one-dimensional configuration which consists of a dielectric lossless slab with a relative permittivity of $\epsilon_r = 4$ and width d embedded in vacuum. The open resonances can be computed in closed form for this example and are given by

$$s_n = \frac{c_0}{4d} \left[\log\left(\frac{1}{9}\right) + 2\pi i n \right] \quad \text{with } n \in \mathbb{Z}. \quad (13)$$

Discretizing the 1D configuration in space and applying the complex scaling method, we obtain a system matrix A with an order $n = 1000$. The eigenvalues of this matrix can be computed directly and a subset of these eigenvalues are shown in Figure 1 (circles) along with a subset of the analytical poles (squares). The latter poles are located on a line parallel to the imaginary axis and all resonances for which the spatial discretization procedure is appropriate are well approximated.

As a second example, we compute the band structure of the simple finite one-dimensional crystal shown in Figure 2. The thickness of the layers is $a_p = 30 \mu\text{m}$ and $b_p = 3 \mu\text{m}$ and the crystal consists of 41 primitive cells. The dielectric layers are lossless and have a relative permittivity of $\epsilon_{r,1} = 3$ and $\epsilon_{r,2} = 1$. It is well known, of course, that if the crystal extends periodically to infinity then its band structure can be computed using the plane wave expansion method (PWE method). This band structure is shown in Figure 3 for an infinite crystal with the same primitive cell as our finite crystal. In Figure 4 we show the bandgap structure of the finite crystal as determined via our Krylov subspace

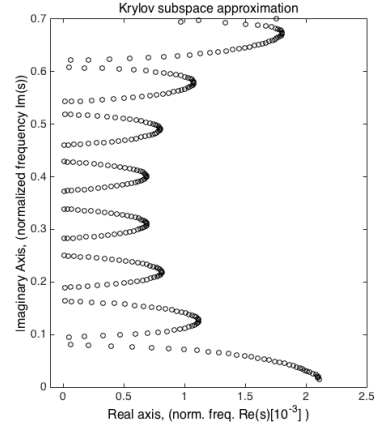


Figure 4: Bandgap structure of the finite 1D photonic crystal. The bandgap structure is computed via Krylov subspace reduction.

reduction technique. We observe that resonances in the middle of a band have higher radiation losses than the resonances located near the edge of a band. The quality factor of resonances near the edge of a band is therefore higher than the quality factor of resonances in the middle of a band.

As a third example, we consider H-polarized electromagnetic fields in a two-dimensional configuration that is invariant in the z -direction. The configuration consists of a square golden object embedded in vacuum (see Figure 5) and a Drude model is used as a constitutive relation for gold with medium parameters $\omega_p = 13.6 \cdot 10^{15} \text{ s}^{-1}$, $\gamma_p = 0.1 \cdot 10^{15} \text{ s}^{-1}$, and $\epsilon_\infty = 1$, while the sidelength of the object is 50 nm. Both the source (cross) and the receiver (triangle) are located outside the object as indicated in Figure 5. The source signature is a derivative of a Gaussian with a maximum in its spectrum at $\lambda_{\text{peak}} = 350 \text{ nm}$ (in vacuum). After the discretization procedure, a semidiscrete Maxwell system with approximately $n = 47000$ time-dependent unknowns is obtained.

Figure 6 shows the reduced-order model of order $m = 6500$ for the magnetic field strength (solid line) at the receiver location and as a function of time. This reduced-order model has essentially converged and coincides with FDTD. Furthermore, using Eq. (12) we can identify the dominant resonant modes that give the largest contribution to the time-domain signal of Figure 6. Taking the first 16 dominant modes into account, the magnetic field response as indicated by the dashed line in Figure 6 is obtained. This result almost completely coincides with the reduced-order model of order 6500 and the FDTD result and illustrates that a small number of resonant modes may give an accurate description of

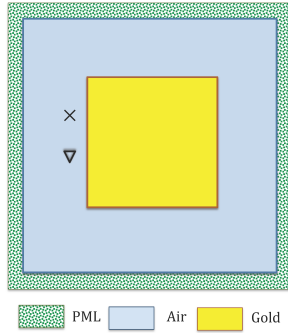


Figure 5: A square golden object embedded in vacuum.

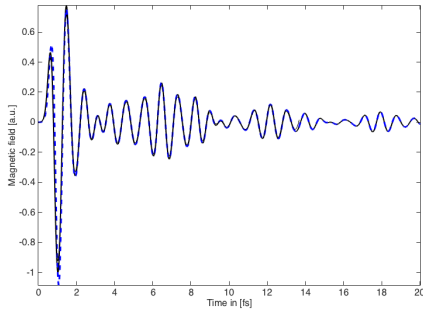


Figure 6: Magnetic field strength at the receiver location as a function of time. Solid line: reduced-order model of order 6500. Dashed line: resonant expansion based on the first 16 dominant resonant modes.

the time-domain magnetic field signal on the time interval of interest. Finally, in Figures 7 and 8 we show the magnitude of the magnetic field strength and the real part of the x -component of the electric field strength of one of the modes that contributes to the time-domain signal. Clearly, these modes are confined to the boundary of the golden object and satisfy the electromagnetic boundary conditions as well.

4 CONCLUSIONS

We have shown that electromagnetic fields on unbounded domains can be efficiently computed via standard Krylov subspace projection techniques. Bandgap structures of finite crystals and dominant resonant modes that are excited by an external source can all be retrieved using a Lanczos-type three-term reduction algorithm both for instantaneously reacting media and media exhibiting relaxation. In future work we will focus on the application of rational Krylov subspace methods, since these methods are expected to provide an additional speedup for inhomogeneous media in general and resonating structures in particular.

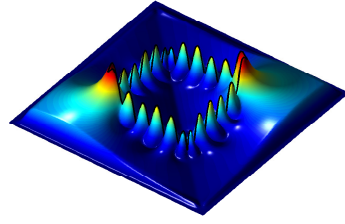


Figure 7: Magnitude of the magnetic field strength of a dominant open resonant mode.

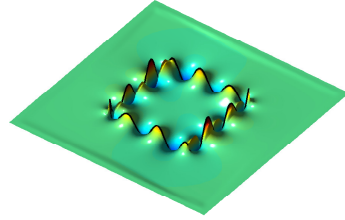


Figure 8: Real part of the x -component of the electric field strength of a dominant open resonant mode.

References

- [1] J. Aguilar and J. M. Combes, “A class of analytic perturbations for one-body Schrödinger Hamiltonians,” *Comm. Math. Phys.*, Vol. 22, 1971, pp. 269 – 279.
- [2] S. Hein, T. Hohage, and W. Koch, “On resonances in open systems,” *J. Fluid Mech.*, Vol. 506, 2004, pp. 255 – 284.
- [3] N. Moiseyev, “Quantum theory of resonances: Calculating energies, widths and cross-sections by complex scaling,” *Phys. Rep.*, Vol. 302, 1998, pp. 211 – 293.
- [4] V. Druskin and R. F. Remis, “A Krylov stability-corrected coordinate stretching method to simulate wave propagation in unbounded domains,” *SIAM J. Sci. Comput.*, Vol. 35, 2013, pp. B376 – B400.
- [5] V. Druskin, S. Güttel, and L. Knizhnerman, “Near-optimal perfectly matched layers for indefinite Helmholtz problems,” *MIMS Eprints 2013.53*, 2014.
- [6] R. F. Remis, “Extended Krylov subspace methods for transient wavefield problems,” *PIERS Online*, Vol. 6, 2010, pp. 455 – 459.
- [7] J. T. Zimmerling, L. Wei, H. P. Urbach, and R. F. Remis, “A Lanczos model-order reduction technique to efficiently simulate electromagnetic wave propagation in dispersive media,” *J. Comput. Phys.*, submitted, 2015.